



# Towards phase pure CZTS thin films by SILAR method with augmented Zn adsorption for photovoltaic applications

Ambily Krishnan<sup>1</sup> · K. Rishad Ali<sup>1</sup> · Geetha Vishnu<sup>1</sup> · Pradeesh Kannan<sup>1</sup>

Received: 3 September 2018 / Accepted: 13 August 2019 / Published online: 22 August 2019  
© The Author(s) 2019

## Abstract

$\text{Cu}_2\text{ZnSnS}_4$  (CZTS) thin films were deposited from a single cationic bath by Successive Ionic Layer Adsorption and Reaction (SILAR) method. Regular SILAR route for CZTS had the drawback of preferential adsorption of copper and tin cations in comparison with zinc. This resulted in  $\text{Cu}_3\text{SnS}_4$  (CTS) and  $\text{Cu}_2\text{S}$  phases rather than phase pure CZTS films. A modified SILAR route, with a separate bath for  $\text{Zn}^{2+}$  ions, circumvented the difficulty and hence led to phase pure CZTS thin films. UV–visible absorption spectra of the CZTS thin films showed absorption coefficients of  $\sim 10^4 \text{ cm}^{-1}$  and a band gap of 1.5 eV. Combined van der Pauw and Hall measurements of CZTS thin films showed a resistivity of approximately  $1.51 \times 10^2 \Omega\text{cm}$ , carrier density of  $\sim 1.28 \times 10^{17} \text{ cm}^{-3}$ , and mobility  $\sim 0.32 \text{ cm}^2 \text{ V}^{-1}\text{s}^{-1}$ . A completely solution processed P–N junction was fabricated and characterized by forming glass/FTO/ $\text{TiO}_2$ /CdS/CZTS multilayer.

**Keywords** SILAR · Solar energy material · Optical band gap · Resistivity · P–N junction

## Introduction

The leading thin film photovoltaic technologies of today based on the chalcogenide materials, cadmium telluride (CdTe) and copper indium gallium selenide (CIGS), are considered to be low cost and widely deployable [1]. But there are some serious concerns regarding both CdTe and CIGS: cadmium is highly toxic, and tellurium, gallium, and indium are extremely rare on our planet. These will make CdTe and CIGS unaffordable in the future and also environmentally unsuitable [2].  $\text{Cu}_2\text{ZnSnS}_{4-x}\text{Se}_x$  (CZTSSe) is a solar cell absorber material similar to CIGS where the scarce element In is replaced by Zn and Ga is replaced by Sn [3]. When the chalcogen is entirely sulfur, we have CZTS which is wholly composed of non-toxic and earth-abundant elements. Thus, CZTS is an earth-abundant alternative with similar processing strategies and challenges as CIGS [4]. The kesterite crystal structure of CZTS is used for photovoltaic applications. CZTS is a *p*-type semi conductor with a direct band gap (1.4–1.5 eV) that matches well with the solar spectrum, has high absorption coefficient (> greater

than  $10^4 \text{ cm}^{-1}$ ) and good electrical properties suitable for photovoltaic applications [3–6].

CZTS has been fabricated by different techniques over the past years. Thermal and electron beam evaporation [7, 8], sputtering [9, 10], and pulsed laser deposition [11] are the various vacuum-based deposition techniques that have been used. But these methods suffer from considerable energy consumption and expensive apparatus requirements. Recent research works in this field are intended to improve the efficiency of CZTS solar cells and reduce production cost by developing several non-vacuum deposition methods. These include spray pyrolysis [12], spin coating [13], chemical bath deposition [14, 15], electro deposition [16], and solvothermal and hot injection methods [17]. The record CZTSSe cell (produced by a hydrazine solution approach) has an efficiency of 12.6% [18], but suffers from large voltage loss due to recombination at defects in the bulk and at the interfaces. This best result was achieved through a Cu-poor, Zn-rich stoichiometry with the band gap being controlled by the S/Se ratio. Major breakthroughs in the development of CZTSSe solar cells depend on finding an alternative back contact that can withstand the full device processing and maintain low series resistance.

With an aim to develop a low cost and industry friendly approach to develop CZTS thin films; we have adopted the Successive Ionic Layer Adsorption and Reaction (SILAR)

✉ Ambily Krishnan  
ambilygvc@gmail.com

<sup>1</sup> Department of Physics, Govt. Victoria College (Affiliated to the University of Calicut), Palakkad, Kerala 678001, India

method which imposes no restrictions on deposition area. In this method, films get deposited by cycles of adsorption and reaction, and this can occur throughout the contact area between the substrate and the liquids (precursor solutions). It is not controlled by external factors like electric or magnetic field, vapor phase transport from source to target, etc. [19, 20]. Also, SILAR method is a room temperature process that is particularly eco-friendly because it uses only non-toxic chemicals and solvents. Traditional single step method [19, 20] as well as stacking of sulfide layers [21, 22] have been used to prepare CZTS films by SILAR so far. Stacking of two layers is more time consuming and difficult for industrial applications. But single step SILAR is extremely challenging for the deposition of quaternary material because of the differential absorptivities of the cations [23, 24].

In the present work, we have attempted depositing CZTS thin films using single step method by widely varying the concentrations of the cationic precursors. A modified SILAR route, by providing a separate bath for  $Zn^{2+}$ , was also attempted. While the former SILAR route resulted in binary and ternary defect phases, latter method led to a phase pure CZTS thin film. A completely solution processed P–N junction with glass/FTO/ $TiO_2$ /CdS/CZTS structure was fabricated and the V–I characteristics were studied. Here, compact  $TiO_2$  was used as a substitute to the usual ZnO window layer. To the best of our knowledge, a completely solution processed P–N junction with a compact  $TiO_2$  window layer for photovoltaics has not been previously reported.

## Experimental

### Materials

Copper (II) chloride ( $CuCl_2 \cdot 2H_2O$ , > 99%), zinc sulfate ( $ZnSO_4 \cdot 7H_2O$ , > 99.5%), tin (II) chloride ( $SnCl_2 \cdot 2H_2O$ , > 97.5%), sodium sulfide ( $Na_2S$ ), cadmium sulfate (99%), and thiourea (99%) were purchased from Merck. Titanium tetrachloride solution (1 M, 99.9%) in toluene was purchased from Sigma-Aldrich. All reagents were used as received. Aqueous solutions were prepared with de-ionized water which was also purchased from Merck.

### Preparation of CZTS films

Substrates (glass slides/FTO-coated glass) were cleaned using de-ionized water, acetone, and iso-propanol by ultrasonication for 10 min each and dried in air, prior to deposition. Initially, deposition was attempted using a single cationic bath. That is, the SILAR cycle involved immersions in four beakers: beaker 1 contained the cationic precursor solution prepared by dissolving copper (II) chloride dihydrate, zinc sulfate heptahydrate, and tin(II) chloride dihydrate

mixed in the molar ratio of 2:1:1 in de-ionized water. Upon dipping, the cations were deposited on to the substrate by adsorption. Thereafter, loosely bound cations were removed by dipping in de-ionized water contained in beaker 2. In beaker 3, 0.16 M  $Na_2S$  solution (having a volume equal to that of the total cationic solution) was used as the anionic precursor. Immersion of the substrates in the anionic solution resulted in reaction of adsorbed cations with the sulfide ions. Deionised water placed in beaker 4 helped in removing the unreacted anions. Dip time in each beaker was optimized as 20 s and the dip and retrieval speeds were both kept at 5 mm per minute. The pH values of the cationic and anionic precursor solutions were precisely controlled and maintained at ~3 and 6, respectively. The experiment was repeated by changing the concentrations of the cationic precursors in the bath. Few examples of the compositional variations in the precursor solutions are as listed in Table 1. Each deposition was carried out by using 50 SILAR cycles.

From Raman analysis and EDS results, it was found that zinc was not incorporated into the films by the above method. So, a separate bath was provided for the  $Zn^{2+}$  ions to enhance its adsorption. The deposition was done using a cycle of six dips as shown in Fig. 1. This enabled  $Zn^{2+}$  cations to get adsorbed onto the substrate surface without facing competition from the copper and tin cations. The concentration of zinc sulfate in its separate neutral bath was 0.2 M. Beaker 4 now contained copper chloride (0.005 M) and tin chloride (0.015 M) with two drops of conc. HCl added to promote complete dissolution of tin chloride. The anionic bath of 0.16 M sodium sulfide solution was acidified with a drop of conc. HCl to help the rapid hydrolysis of sodium sulfide giving  $S^{2-}$  ions. The dip time and speeds were the same as mentioned earlier.

### Fabrication of P–N junction

A compact layer of  $TiO_2(c-TiO_2)$  was deposited over FTO-coated glass substrate by hydrolysis of 0.1 M aqueous  $TiCl_4$  solution and annealing at 500 °C for an hour. CdS thin films were deposited over the  $TiO_2$  film by chemical bath deposition method. For this, we used aqueous solutions of 2.5 mM  $CdSO_4 \cdot 8/3 H_2O$  and 0.06 M

**Table 1** Composition of the precursor solutions of the films deposited from single cationic bath

Film name	Cu/(Zn+Sn) ratio	Zn/Sn ratio
St.	1	1
A	0.7	1.15
B	0.6	1.15
C	0.8	1.15
D	0.7	1.25

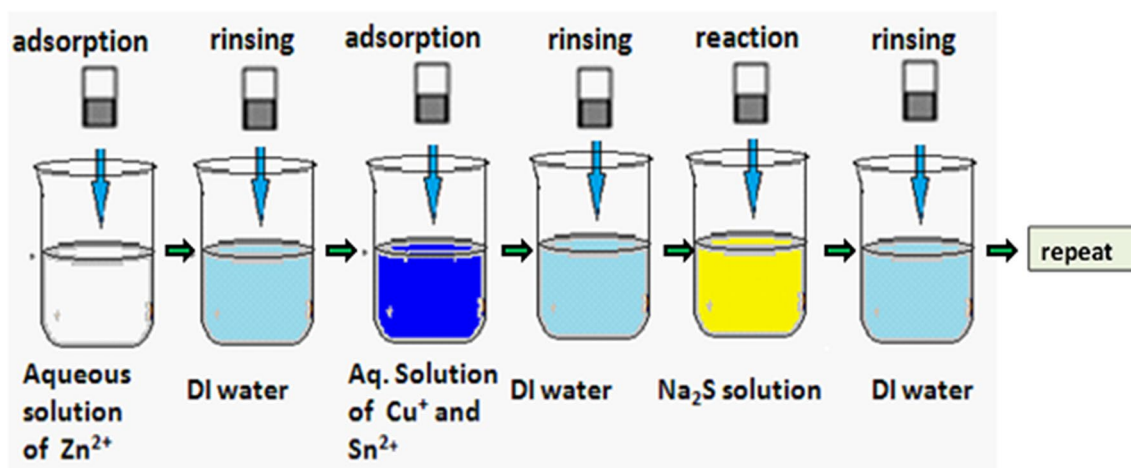


Fig. 1 Six dip SILAR cycle giving augmented Zn adsorption

thiourea with adequate amounts of ammonia solution and few drops of TEA. The deposition was done at 65 °C for 15 min [25]. Over the CdS film, CZTS was deposited by the six dip SILAR cycle described above. Forty cycles were given with dip time of 20 s in each solution, and dip and retrieval speeds of 5 and 2 mm per minute, respectively. The glass/FTO/TiO<sub>2</sub>/CdS/CZTS combination was annealed at 200 °C for an hour.

## Characterization

Structural characterization and phase formation of the SILAR-deposited films and compact TiO<sub>2</sub> layer were done using Raman spectroscopy (Renishaw inVia confocal Raman microscope, using excitation wavelength of 532 nm with spot size of 1 μm). Formation of nano crystalline CdS thin films was confirmed by X-ray diffraction (Bruker AXS D8 Advance X ray diffractometer using Cu-K<sub>α</sub> X-rays of wavelength 1.5406 Å) and Raman analysis. Surface morphology of the films was studied using Field Emission Scanning Electron Microscopy (FESEM) (JEOL JSM 6390). Thickness of the films was measured by interferometry/cross-section FESEM and refractive indices by Brewster angle method [26, 27]. The optical properties were studied using UV–visible spectroscopy (Model: Varian Cary-5000) and band gap was determined from the Tauc plots. Electrical measurements were done by four probe method using Keithley SMU 2450. The *p*-type conductivity was confirmed by hot-probe method. Atomic Force Microscopy (AFM) (AFM-A-100 SPM) was used to determine the surface roughness of the CZTS films. V-I characterization of the junction was performed using Keithley 2450 SMU by four probe method.

## Results and discussion

### Structural properties

Figure 2 shows the Raman spectra of the as-deposited films obtained by SILAR. Raman spectra of the films deposited using single cationic bath revealed major peaks around 319 cm<sup>-1</sup> and 475 cm<sup>-1</sup> (curves A, B, C, D and St of Fig. 2a). These indicated the formation of Cu<sub>3</sub>SnS<sub>4</sub> (CTS) and Cu<sub>2</sub>S, respectively, rather than CZTS. It means that zinc has not been adsorbed, and copper and tin are the major cations present in the deposited films. When a separate cationic bath was used for zinc, the Zn content improved considerably and the Raman peaks characteristic of Cu<sub>2</sub>ZnSnS<sub>4</sub> were obtained (Fig. 2b). The deconvoluted Raman spectrum shows the peak at 331 cm<sup>-1</sup> corresponding to the standard value of 335 cm<sup>-1</sup> due to the A<sub>1</sub> vibrational mode of the CZTS molecule where the anions vibrate towards the *z*-axis. The peaks at 275 cm<sup>-1</sup>, 292 cm<sup>-1</sup>, and 342 cm<sup>-1</sup> correspond to the values at 278, 290, and 341 cm<sup>-1</sup> due to the E vibrational modes of kesterite crystal structure of Cu<sub>2</sub>ZnSnS<sub>4</sub>. The peak at 292 cm<sup>-1</sup> might also be due to the B symmetry mode (285 cm<sup>-1</sup>) corresponding to movements of the Cu/Zn and Cu/Sn atomic planes [28–30]. The peaks at 319 cm<sup>-1</sup> and 475 cm<sup>-1</sup> due to the CTS and Cu<sub>2</sub>S defect phases are absent, now showing the formation of pure CZTS phase in the thin film formed. Deviation from standard values must be due to the strain produced in the films during solvent evaporation.

Formation of TiO<sub>2</sub> with anatase crystal structure was also confirmed using Raman spectroscopy (Fig. 2c). The sharp peak at 144 cm<sup>-1</sup> is due to the vibrations of the Ti–Ti covalent bond. The formation of CdS film was

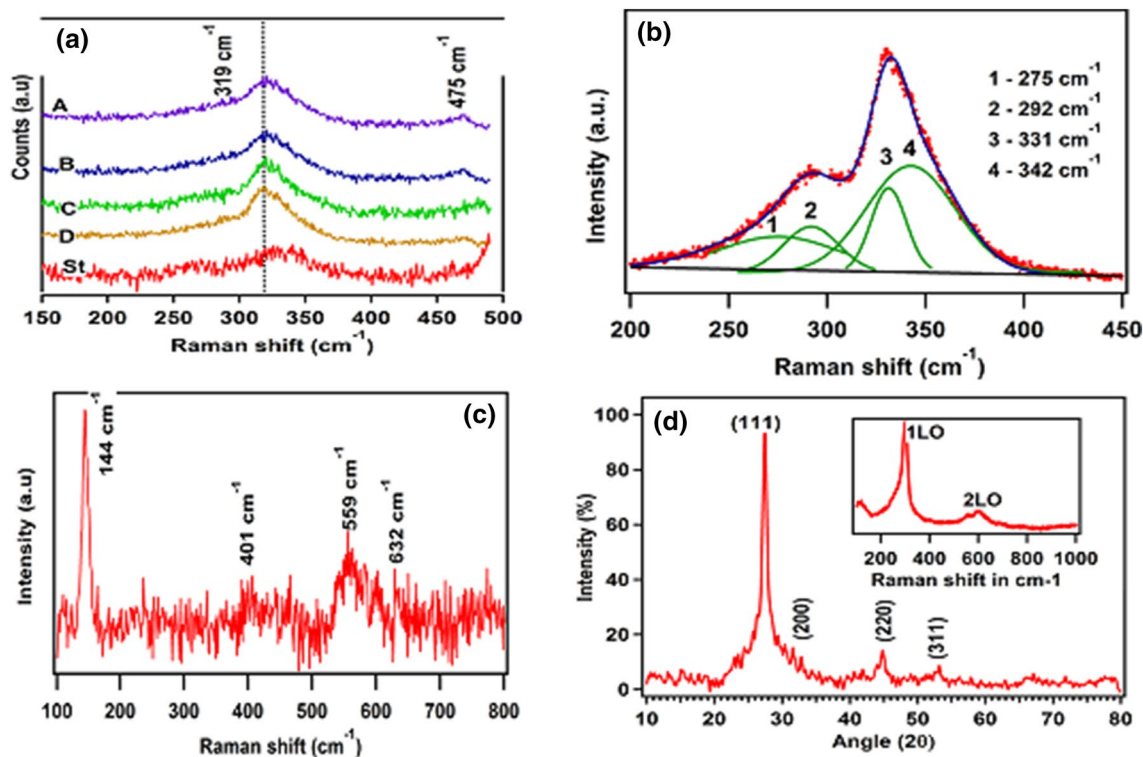


**Fig. 2** **a** Raman spectra of the films deposited using single cationic bath. **b** Raman spectrum of CZTS film deposited by SILAR with augmented Zn adsorption. **c** Raman spectrum of compact  $\text{TiO}_2$  film. **d** XRD pattern of CdS film and Raman spectrum as inset

confirmed by X-ray diffraction and Raman spectroscopy. The XRD pattern of CdS film (Fig. 2d) showed a sharp peak at  $27.43^\circ$  and smaller peaks at  $44.8^\circ$  and  $53.15^\circ$ . These show reflections from the (111), (220), and (311) planes of cubic crystal structure of CdS. Raman spectra of the CdS films showed a major peak at  $300\text{ cm}^{-1}$  and a smaller peak at  $600\text{ cm}^{-1}$ . These are due to the first- and second-order longitudinal optic (LO) phonon modes of CdS (inset of Fig. 2d).

The surface morphology of the CZTS films deposited on glass substrate was studied using FESEM and AFM (Fig. 3a). The FESEM micrographs revealed a dense morphology with globular structures of average size 100 nm (Fig. 3b). The AFM data (Fig. 3c) showed an average surface roughness of 66 nm for a 216 nm thick film (measured by optical interferometric method) deposited by 40 SILAR cycles. The growth rate of the films was  $\sim 6\text{ nm/cycle}$ .

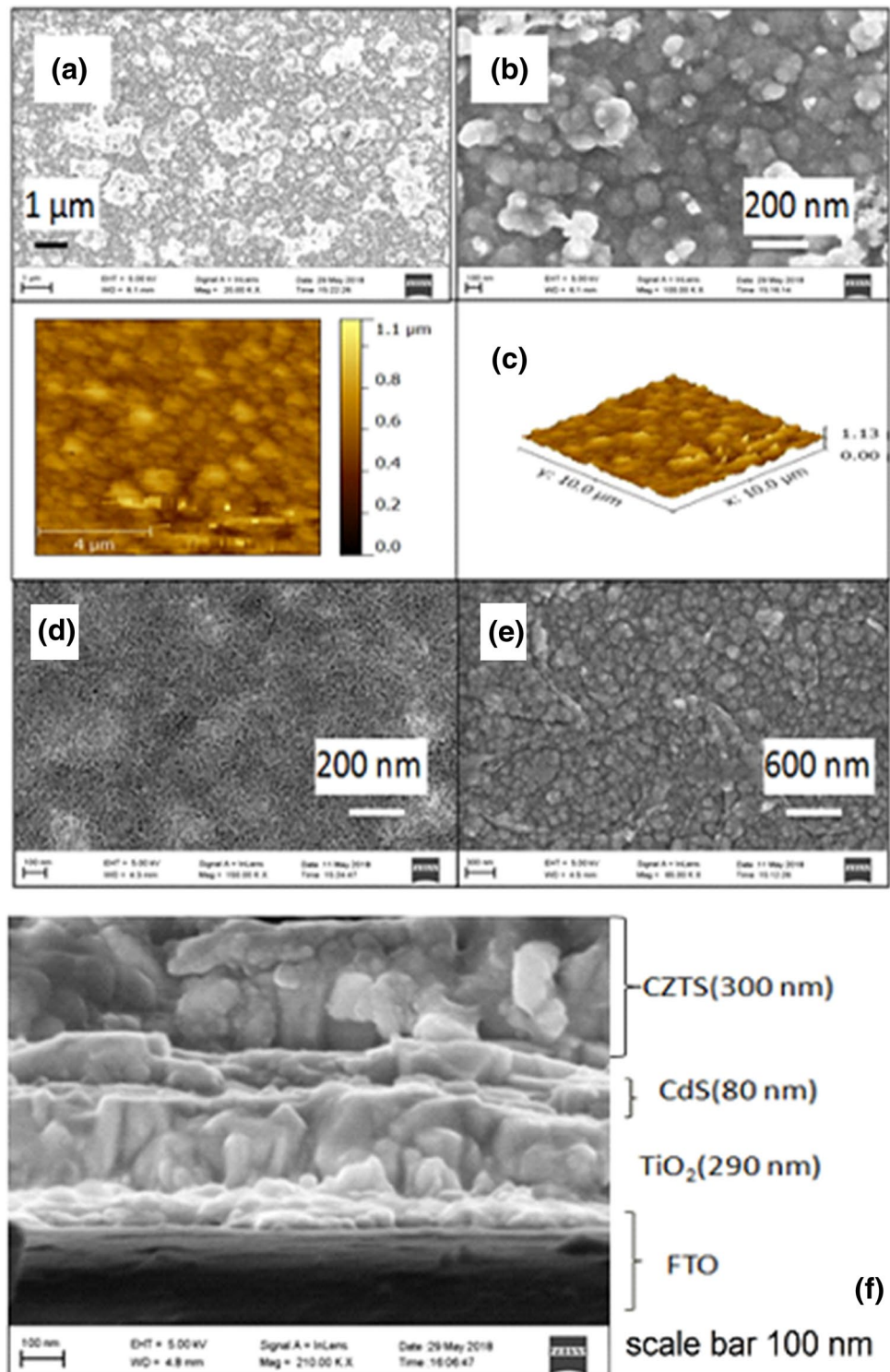
Figure 3d shows the FESEM image of c- $\text{TiO}_2$  film and Fig. 3e that of CdS film coated over c- $\text{TiO}_2$  layer. The dense packing of the nano crystalline  $\text{TiO}_2$  layer and the uniformly formed cadmium sulfide grains over it are clear from these micrographs. Figure 3f shows the FESEM image of the cross section of glass/FTO/ $\text{TiO}_2$ /CdS/CZTS heterostructure. Approximate thickness of different layers estimated from the cross-sectional SEM image is  $\text{TiO}_2 \sim 290\text{ nm}$ , CdS  $\sim 80\text{ nm}$ , and CZTS  $\sim 300\text{ nm}$ .

## Optical and electrical properties

Thickness of the films was measured by interferometry (Fizeau fringes) by forming a wedge-shaped air film between two optical flats, one carrying the deposited film. Sodium light was used as source for forming the interference pattern. The step width  $s$  and band width  $\beta$  of the fringe patterns were measured using an optical microscope and film thickness calculated using formula  $t = \frac{s\lambda}{2\beta}$ . For the CZTS film deposited by 40 cycles of SILAR with augmented zinc adsorption, it was measured to be 216 nm. Refractive indices, estimated from Brewster angle measurements, of the CZTS,  $\text{TiO}_2$  and CdS films are 2.90, 2.38, and 2.31, respectively.

The reflectance, transmittance, and absorbance of the films coated on glass were measured in the wavelength range 300 nm to 900 nm. The CZTS film has a broad absorption band with absorption coefficient lying in the  $10^4\text{ cm}^{-1}$  range. CZTS is a direct band gap material and for allowed transitions,  $ah\nu = A\sqrt{(h\nu - E_g)}$ , where  $\alpha$  is the absorption coefficient,  $A$  a constant, and  $E_g$  is the optical band gap. To find the optical band gaps of the deposited films,  $(ah\nu)^2$  was plotted against  $h\nu$  (Tauc plots) and energy gaps were determined as the  $x$ -intercepts at zero absorption obtained by fitting straight lines (Fig. 4a). The

**Fig. 3** **a** and **b** FESEM micrographs of CZTS film deposited on glass substrate. **c** AFM image of CZTS film. **d** FESEM image of c-TiO<sub>2</sub> film. **e** FESEM image of CdS film coated over c-TiO<sub>2</sub> layer. **f** FESEM micrograph of cross section of P–N junction with structure glass/FTO/TiO<sub>2</sub>/CdS/CZTS



band gap of CZTS thin film coated on glass was estimated as 1.50 eV. The high absorption coefficient and optimum energy gap show that the film can act as a good absorber layer for solar cells enabling efficient photon absorption and subsequent electron hole pair generation.

The optical properties of the TiO<sub>2</sub> and CdS films were also measured using UV–visible spectroscopy. The TiO<sub>2</sub> films showed good transmittance of over 80% over the entire visible and IR range while CdS absorbed blue regions of the visible spectrum, thereby reducing the transmittance there

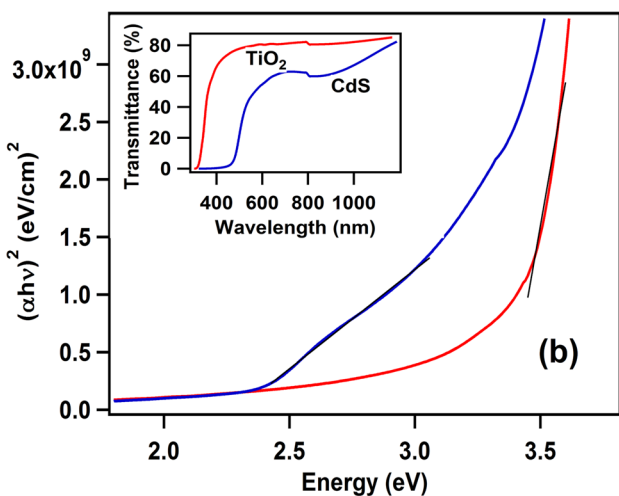
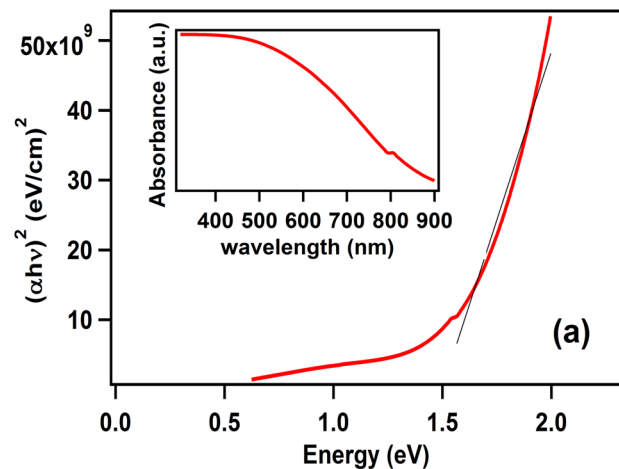


**Fig. 4** **a** Tauc plot and absorbance spectrum (inset) of CZTS film deposited on glass. **b** Tauc plots and transmittance spectrum (inset) of CdS and c-TiO<sub>2</sub> films deposited on glass substrates

(inset of Fig. 4b). The Tauc plot of CdS film gave a direct band gap of 2.37 eV while that of TiO<sub>2</sub> showed a band gap of 3.32 eV (Fig. 4b). Optical properties of these films are extremely important when they are used as window layers in solar cells. The present study shows that the combination of compact TiO<sub>2</sub> and CdS thin films can be successfully employed in thin film solar cells instead of the usual ZnO/CdS layers without affecting the transparency to incident light.

The electrical properties of the CZTS films were measured by using a combination of van der Pauw and Hall techniques. The *p*-type conductivity was confirmed by hot-probe method. The values of resistivity, carrier concentration, and mobility were found to be approximately  $1.51 \times 10^2 \Omega\text{cm}$ ,  $1.28 \times 10^{17} \text{cm}^{-3}$ , and  $0.32 \text{cm}^2 \text{V}^{-1}\text{s}^{-1}$ , respectively. The poor mobility may be attributed to the small grain size of the film. This leads to recombination of the electrons and holes

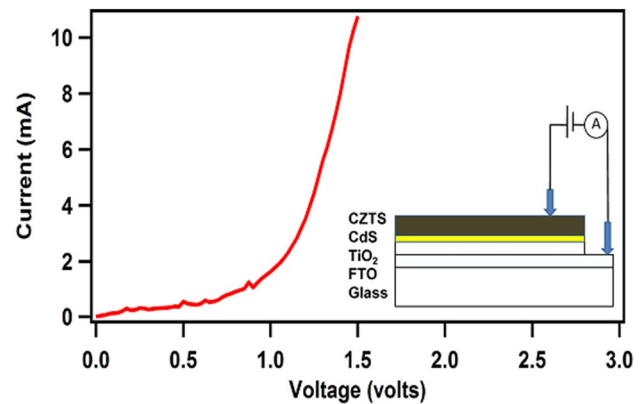


**Fig. 5** Schematics and dark V–I characteristics of CZTS/CdS/TiO<sub>2</sub>/FTO P–N junction

at the grain boundaries. Recombination can be minimized by improving the grain size of the film. Electrical measurements were performed with films coated on glass substrates. In actual devices, the films would either be coated over conducting substrates or over *n*-type buffer layers. The electrical properties of the absorbing films will then be surely different from those tabulated above. In any case, recombination of the charge carriers at the grain boundaries leading to poor mobility will affect the solar cell performance.

### P–N junction V–I characteristic

We have constructed a P–N junction by following the superstrate configuration commonly used for CdTe solar cells instead of following the traditional glass/Mo/CZTS/CdS substrate configuration used for CIGS and CZTS solar cells. Only the P–N junction has been fabricated and not the complete solar cell. The V–I characteristic of the junction measured in dark is as shown in Fig. 5. The curve gave a knee voltage near 1 V showing that a good  $V_{oc}$  can be expected from a solar cell constructed with glass/FTO/TiO<sub>2</sub>/CdS/CZTS structure developed by this low cost and industry friendly method. This is because the dark (recombination) current is negligibly small for voltages lower than 1 V which in turn will give rise to higher  $V_{oc}$  since  $V_{oc} = kT/q \ln(I_L/I_0 + 1)$ , where  $I_L$  is the light generated current and  $I_0$  is the recombination current. Theoretically, the upper limit of  $V_{oc}$  is decided by the band gap energy of the material. But practically  $V_{oc}$  is lower than the limit set by band gap. This is because solar cell needs to be contacted to collect the excited charge carriers. The difference in potential level of the contacts then sets an upper limit for  $V_{oc}$ . For higher  $V_{oc}$ ,  $I_0$  should be lower and the series resistance imposed by the contacts is low. The compact TiO<sub>2</sub> layer serves as an electron transport layer as well as a window layer for light while CdS acts as the *n*-type buffer layer forming a good P–N junction

at the interface. Without the TiO<sub>2</sub> layer, chances of CZTS layer getting shorted to the FTO layer beneath are high. This shows that TiO<sub>2</sub> film serves the same purpose here as the compact hole blocking layer in perovskite solar cells. The combination provides maximum photon transmission to the absorber layer and facilitates the deposition of phase pure CZTS over it. To complete a solar cell device, electrode metal layers have to be deposited over the CZTS thin film so that the separated charge carriers can be collected and supplied to the external circuit. This can be done without shorting of the junction only if the CZTS film is free of pin holes and compact. Efforts are in progress to achieve such photovoltaic device quality thin films.

## Conclusion

Uniform thin films of CZTS have been deposited by room temperature single step SILAR process by properly controlling the precursor concentrations and using a separate cationic bath for Zn<sup>2+</sup> ions. Repetition of the six dip SILAR process with augmented zinc adsorption yielded uniform CZTS thin films with good light absorbing and electrical properties. The CZTS thin films had absorption coefficients of the order of 10<sup>4</sup> cm<sup>-1</sup> and a band gap of 1.5 eV. CZTS thin films deposited on glass substrates showed a resistivity of approximately 1.51 × 10<sup>2</sup> Ωcm, carrier density of ~ 1.28 × 10<sup>17</sup> cm<sup>-3</sup>, and mobility ~ 0.32 cm<sup>2</sup> V<sup>-1</sup>s<sup>-1</sup>. A completely solution processed P–N junction with structure glass/FTO/TiO<sub>2</sub>/CdS/CZTS was fabricated and its knee voltage was estimated to be near 1 V from the V–I characteristics. Combined with the non-toxic nature and earth abundance of the constituent elements, the industry friendly low temperature SILAR method to deposit CZTS is sure to reduce the cost of the thin film photovoltaic device. The combination of compact TiO<sub>2</sub> as window layer, CdS buffer layer, and CZTS absorber layer can be used to make solar cells with improved V<sub>oc</sub>, provided we are able to get pin hole-free absorber layers and good electrode metal layer over it for ohmic contacts.

**Acknowledgements** The authors wish to thank T.N. Narayanan of TIFR, Hyderabad for Raman Spectroscopy, STIC and Dept. of Physics, Cochin University of Science and Technology for UV–visible spectroscopy, SEM and IUCNN, Mahatma Gandhi University for AFM of the samples. The authors acknowledge Department of Science and Technology, Govt. of India for providing funding under DST-FIST scheme. The first author acknowledges the University Grants Commission, India for providing assistance under Faculty Development Program.

**Open Access** This article is distributed under the terms of the Creative Commons Attribution 4.0 International License (<http://creativecommons.org/licenses/by/4.0/>), which permits unrestricted use, distribution, and reproduction in any medium, provided you give appropriate credit to the original author(s) and the source, provide a link to the Creative Commons license, and indicate if changes were made.

## References

- Green, M.A.: Thin-film solar cells: review of materials, technologies and commercial status. *J. Mater. Sci.: Mater. Electron.* **18**(1), 15–19 (2007)
- Lee, T.D., Ebong, A.U.: A review of thin film solar cell technologies and challenges. *Renew. Sustain. Energy Rev.* **70**, 1286–1297 (2017)
- Mitzi, D.B., Gunawan, O., Todorov, T.K., Wang, K., Guha, S.: The path towards a high-performance solution-processed kesterite solar cell. *Sol. Energy Mater. Sol. Cells* **95**(6), 1421–1436 (2011)
- Suryawanshi, M.P., Agawane, G.L., Bhosale, S.M., Shin, S.W., Patil, P.S., Kim, J.H., Moholkar, A.V.: CZTS based thin film solar cells: a status review. *Mater. Technol.* **28**(1–2), 98–109 (2013)
- Abermann, S.: Non-vacuum processed next generation thin film photovoltaics: towards marketable efficiency and production of CZTS based solar cells. *Sol. Energy* **94**, 37–70 (2013)
- Wallace, S.K., Mitzi, D.B., Walsh, A.: The steady rise of Kesterite solar cells. *ACS Energy Lett.* **2**(4), 776–779 (2017)
- Katagiri, H., Saitoh, K., Washio, T., Shinohara, H., Kurumadani, T., Miyajima, S.: Development of thin film solar cell based on Cu<sub>2</sub>ZnSnS<sub>4</sub> thin films. *Sol. Energy Mater. Sol. Cells* **65**(1–4), 141–148 (2001)
- Mkawi, E.M., Al-Hadeethi, Y., Shalaan, E., Bekyarova, E.: Substrate temperature effect during the deposition of (Cu/Sn/Cu/Zn) stacked precursor CZTS thin film deposited by electron-beam evaporation. *J. Mater. Sci.: Mater. Electron.* **29**(23), 20476–20484 (2018)
- Tanaka, T., Nagatomo, T., Kawasaki, D., Nishio, M., Guo, Q., Wakahara, A., Yoshida, A., Ogawa, H.: Preparation of Cu<sub>2</sub>ZnSnS<sub>4</sub> thin films by hybrid sputtering. *J Phys Chem Solids* **66**(11), 1978–1981 (2005)
- Katagiri, H., Jimbo, K., Maw, W.S., Oishi, K., Yamazaki, M., Araki, H., Takeuchi, A.: Development of CZTS-based thin film solar cells. *Thin Solid Films* **517**(7), 2455–2460 (2009)
- Shin, B., Gunawan, O., Zhu, Y., Bojarczuk, N.A., Chey, S.J., Guha, S.: Thin film solar cell with 8.4% power conversion efficiency using an earth-abundant Cu<sub>2</sub>ZnSnS<sub>4</sub> absorber. *Prog. Photovolt.: Res. Appl.* **1**, 72–76 (2013)
- Mahjoubi, S., Bitri, N., Abaab, M., Ly, I.: Effect of copper concentration on the characteristics of Cu<sub>2</sub>ZnSnS<sub>4</sub> (CZTS) thin films. *Mater. Lett.* **216**, 154–157 (2018)
- Moritake, N., Fukui, Y., Oonuki, M., Tanaka, K., Uchiki, H.: Preparation of Cu<sub>2</sub>ZnSnS<sub>4</sub> thin film solar cells under non-vacuum condition. *Phys. Status Solidi (c)* **6**(5), 1233–1236 (2009)
- Wangperawong, A., King, J.S., Herron, S.M., Tran, B.P., Pangan-Okimoto, K., Bent, S.F.: Aqueous bath process for deposition of Cu<sub>2</sub>ZnSnS<sub>4</sub> photovoltaic absorbers. *Thin Solid Films* **519**, 2488–2492 (2011)
- Cao, M., Li, L., Zhang, B.L., Huang, J., Wang, L.J., Shen, Y., Sun, Y., Jiang, J.C., Hu, G.J.: One-step deposition of Cu<sub>2</sub>ZnSnS<sub>4</sub> thin films for solar cells. *Sol. Energy Mater. Sol. Cells* **117**, 81–86 (2013)
- Scragg, J.J., Berg, D.M., Dale, P.J.: A 3.2% efficient Kesterite device from electrodeposited stacked elemental layers. *J. Electroanal. Chem.* **646**(1–2), 52–59 (2010)
- Zhou, H., Hsu, W.C., Duan, H.S., Bob, B., Yang, W., Song, T.B., Hsu, C.J., Yang, Y.: CZTS nanocrystals: a promising approach for next generation thin film photovoltaics. *Energy Environ. Sci.* **6**(10), 2822–2838 (2013)
- Wang, W., Winkler, M.T., Gunawan, O., Gokmen, T., Todorov, T.K., Zhu, Y., Mitzi, D.B.: Device characteristics of CZTSSe thin-film solar cells with 12.6% efficiency. *Adv. Energy Mater.* **4**(7), 1301465 (2014)

19. Mali, S.S., Shinde, P.S., Betty, C.A., Bhosale, N., Oh, Y.W., Patil, P.S.: Synthesis and characterization of Cu<sub>2</sub>ZnSnS<sub>4</sub> thin films by SILAR method. *J. Phys. Chem. Solids* **73**(6), 735–740 (2012)
20. Shinde, N.M., Dubal, D.P., Dhawale, D.S., Lokhande, C.D., Kim, J.H., Moon, J.H.: Room temperature novel chemical synthesis of Cu<sub>2</sub>ZnSnS<sub>4</sub> absorbing layer for photovoltaic application. *Mater. Res. Bull.* **47**(2), 302–307 (2012)
21. Su, Z., Yan, C., Sun, K., Han, Z., Liu, F., Liu, J., Lai, Y., Li, J., Liu, Y.: Preparation of Cu<sub>2</sub>ZnSnS<sub>4</sub> thin films by sulfurizing stacked precursor thin films via successive ionic layer adsorption and reaction method. *Appl. Surf. Sci.* **258**(19), 7678–7682 (2012)
22. Suryawanshi, M.P., et al.: Improved photoelectrochemical performance of Cu<sub>2</sub>ZnSnS<sub>4</sub> (CZTS) thin films prepared using modified successive ionic layer adsorption and reaction (SILAR) sequence. *Electrochim. Acta* **150**, 136–145 (2014)
23. Ma, S., Sui, J., Cao, L., Li, Y., Dong, H., Zhang, Q., Dong, L.: Synthesis of Cu<sub>2</sub>ZnSnS<sub>4</sub> thin film through chemical successive ionic layer adsorption and reactions. *Appl. Surf. Sci.* **349**, 430–436 (2015)
24. Mahajan, S., Stathatos, E., Huse, N., Birajdar, R., Kalarakis, A., Sharma, R.: Low cost nanostructure kesterite CZTS thin films for solar cells application. *Mater. Lett.* **210**, 92–96 (2018)
25. Krishnan, A., Vishnu, G., Kannan, P.: Rapid microwave synthesis of Cu<sub>2</sub>ZnSnS<sub>4</sub> nanocrystals for photovoltaic junctions. *Int. J. Energy Res.* **43**(1), 589–595 (2019)
26. Chopra, K.L.: *Thin Film Phenomena*. Mc Graw Hill Book Company, New York (1969)
27. Subrahmanyam, N., Lal, Brij, Avadhanulu, M.N.: *Optics*. S. Chand & Co., New Delhi (1994)
28. Ghediya, Prashant R., Chaudhuri, Tapas K.: Microwave-processed copper zinc tin sulphide (CZTS) inks for coatings in solar cells. In: Zhang, J., Jung, Y.G. (eds.) *Advanced Ceramic and Metallic Coating and Thin Film Materials for Energy and Environmental Applications*, pp. 121–174. Springer, Switzerland (2018)
29. Berg, D.M., Arasimowicz, M., Djemour, R., Gütay, L., Siebentritt, S., Schorr, S., Fontané, X., Izquierdo-Roca, V., Pérez-Rodríguez, A., Dale, P.J.: Discrimination and detection limits of secondary phases in Cu<sub>2</sub>ZnSnS<sub>4</sub> using X-ray diffraction and Raman spectroscopy. *Thin Solid Films* **569**, 113–123 (2014)
30. Kodigala, S.R.: *Thin film solar cells from earth abundant materials: growth and characterization of Cu<sub>2</sub>(ZnSn)(SSe) 4 thin films and their solar cells*. Elsevier Inc., Amsterdam (2013)

**Publisher's Note** Springer Nature remains neutral with regard to jurisdictional claims in published maps and institutional affiliations.